Subsurface geological structure and tectonics as evidenced from integrated interpretation of aeromagnetic and remote sensing data over Kutch sedimentary basin, western India

P. Chandrasekhar[1,*], K. Chandra Mouli[2], D. P. Rao[3] and V. K. Dadhwal[4]

[1]National Remote Sensing Centre, Indian Space Research Organisation, Hyderabad 500 037, India
[2]F. No. 505, Prashant Towers, Alkapuri, Hyderabad 500 035, India
[3]F. No. 402, Manasasarovar Apartment, Kalyan Nagar, Hyderabad 500 038, India
[4]Indian Institute of Space Science and Technology, Thiruvananthapuram 695 547, India

A number of magnetic zones, faults, lineaments and domal structures were interpreted based on the analysis of aeromagnetic data. Magnetic basement depth and thickness of the sediments were computed by means of quantitative interpretation techniques. A number of alternate basement ridges/highs/uplifted blocks and depressions/lows/downthrown blocks were also delineated. The lithological variations, major folding and faulting patterns, circular spectral anomalies and other geological structures were interpreted from IRS-1C satellite data. The tectonic framework and deformational history of the basin were deduced. The results obtained from the interpretation of aeromagnetic and satellite data were then integrated and the potential zones of hydrocarbon deposits and vulnerable areas for earthquake occurrence were derived.

Keywords: Aeromagnetic and satellite data, basement depth, hydrocarbons, earthquakes.

THE sedimentary basin of Kutch Gujarat (Figure 1) has a great economic and tectonic significance. This area has potential for oil and gas reserves, as the basin is contiguous to the hydrocarbon-producing Cambay basin in the east and southeast, Mumbai offshore basin in the south, and the south Indus basin of Pakistan in the north, where a number of oil and gas fields have already been discovered. Exploratory efforts have led to the discovery of oil and gas deposits in the offshore areas as well. A total of 29 exploratory wells have already been drilled in and around the study area in the approximate depth range 1200–4600 m, and oil and gas strikes were observed in most of them (http://www.dghindia.org/17.aspx; https://www.google.co.in/?gfe_rd=cr&ei=TDJ5VcuuCerI8AeLrLmoCg&gws_rd=ssl#q=Kutch++geological+maps). Kutch basin also falls in Zone V of the Seismic Zonation Map of India (http://www.imd.gov.in/section/seismo/static/seismo-zone.htm), indicating highest risk for earthquakes; it is the only such zone outside the Himalayan seismic belt. The major earthquake at Bhuj of magnitude 7.7 (on 26 January 2001) had rocked this area and the surroundings in the morning at 08 : 46 h and, subsequently a number of aftershocks were also reported[1–3] (http://www.isr.gujarat.gov.in/latest_eq.php; http://pubs.er.usgs.gov/publication/70025930). The major earthquake of Nepal that occurred on 25 April 2015 with a magnitude of 7.8 also affected this area causing tremors of magnitude >4 on the Richter scale (http://www.isr.gujarat.gov.in/latest_eq.php), probably due to its relation with Delhi–Aravalli belt (https://www.google.co.in/webhp?sourceid=chrome-instant&ion=1&espv=2&ie=UTF-8#q=gravity%20image%20map%20of%20india).

Kutch region is geologically well known for its Mesozoic and Tertiary sediments (Figure 1) and is well documented[4–11]. From a previous study of the basin, it was found that the stratigraphy comprises strata ranging in age from the Lower Jurassic to Holocene, and the complete sequence is exposed only in the Kutch mainland. The older Mesozoic sequence is exposed in Pachham, Khadir, Bela and Chorar islands to the north of Kutch mainland, whereas the strata of intermediate age of Mesozoic sequence are in the Wagad Highland. The Tertiary rocks are exposed in the peripheral plains of these Highlands. The extensive flows of Deccan Traps representing volcanic activity in this region had terminated the Mesozoic sedimentation during Late Cretaceous to Early Palaeocene[10]. Deccan Trap lava flows of Late Cretaceous to Early Palaeocene divide the Mesozoic and Tertiary stratigraphy of the Kutch region (http://www.jsce.or.jp/report/12/Indian/Report/PDF/indo3.pdf).

Oil and gas reserves form due to compaction and disintegration process of organic material resulting from syn-sedimentary poly-phase tectonic deformations. This tectonic framework, apart from the resource formation, is also responsible for triggering earthquakes. Thus the causative environment for hydrocarbons and earthquakes

*For correspondence. (e-mail: chandrasekhar_p@nrsc.gov.in)

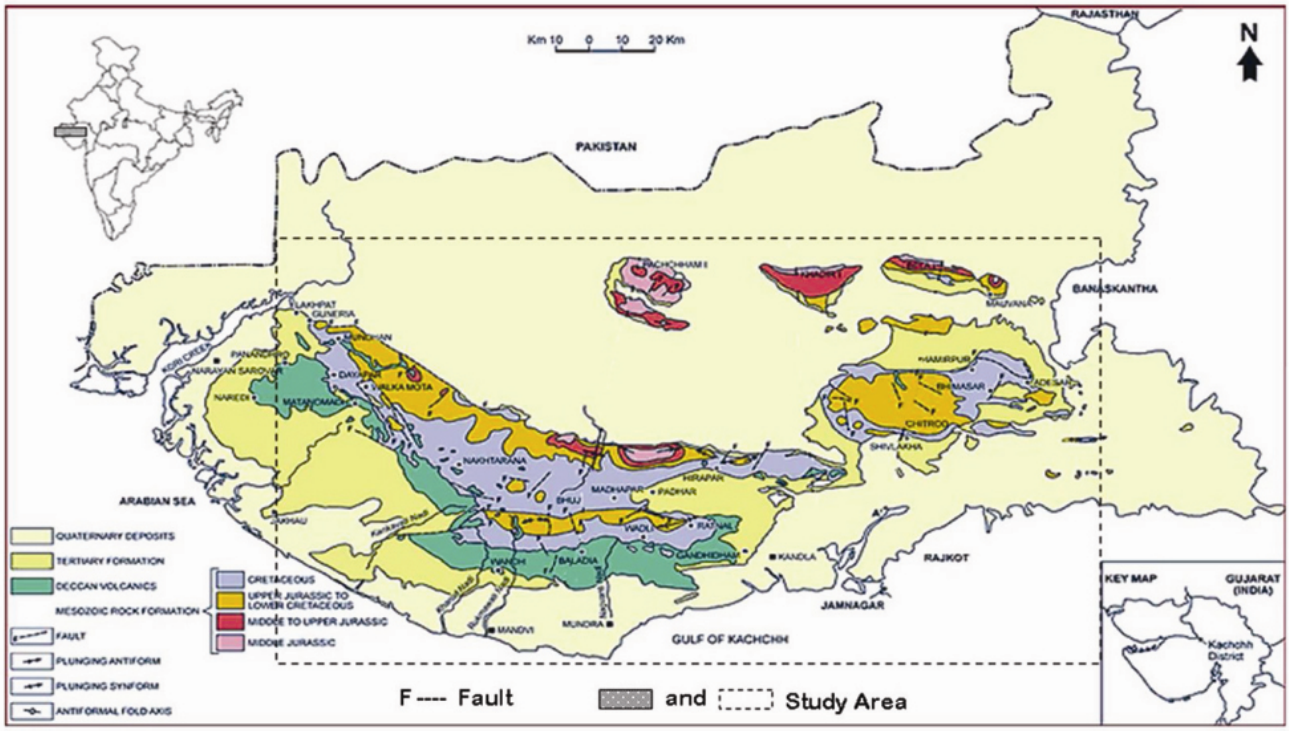

Figure 1. Geological map of the study area (source: Geological Survey of India).

is essentially governed by the subsurface geological structure and tectonics. The fact that most of the subsurface rocks have magnetic susceptibility makes the magnetic method one of the best for oil and gas exploration and earthquake studies[12]. In comparison with the basement rock (igneous/metamorphic), the magnetism of the overlying sedimentary rocks is negligible, making it possible to map the lateral and vertical boundaries of the sedimentary basin and estimate the thickness of the sediments, which are vital in hydrocarbons exploration[13,14]. Aeromagnetic data are also used for mapping deep-rooted faults and lineaments and computing their depths, which are responsible for the release of seismic energy during earthquake events[15]. On the other hand, the geological structures can also be interpreted from the space-based multispectral satellite data[12,16–19]. Remote sensing, however, suffers from the limitation of mapping the geology in the vertical/depth section and also when the terrain is covered with different types of land use. Hence, in the present study the electromagnetic spectral anomalies were corroborated, correlated and integrated with the potential field anomalies of the aeromagnetic data in order to overcome the inherent ambiguity in interpretation, and thus a comprehensive subsurface geological model was derived.

Remote sensing data interpretation

Interpreting Indian Remote Sensing (IRS 1C) satellite data of LISS III sensor with a spatial resolution of 23.5 m, the geological features exhibiting typical spectral signatures were interpreted based on the image elements and geotechnical evidences[18,20] (Figure 2). Faults were interpreted as anomalous truncations/offsets of formations/sharp topographic breaks/dislocations of the linear anomaly trends. Lineaments were interpreted based on their characteristic tonal variations, spatial relationship with other geological units, linear alignment of streams, water bodies and vegetation. The geomorphic anomaly appearing in the form of a domal structure was interpreted based on the identification of circular anomalies and circular drainage pattern, all along the above structure, besides a number of circular spectral anomalies with typical tonal variations, terrain morphology, smooth texture and drainage anomalies. A big shear zone in the western portion lying at the contact of Deccan Trap with Bhuj Formation, passing through Nakhtarana trending in NW–SE direction, was also brought out in addition to a number of fault trends. Two major fault systems were interpreted: (i) strike–slip faults: E–W (denoted as 'S1') and ENE–WSW (denoted as 'S2'), as evidenced from the displacements of the formation and (ii) high-angle oblique faults: NE–SW (denoted as 'S1^1') and NW–SE (denoted as 'S2^1'), as they are segmenting and displacing the strike–slip faults. In the Kutch mainland, S1 faults show a swing to NW–SE direction in the central and northern sides of the western part, except a SW swing in the southern side. Similarly, S1^1 faults in the entire study area are not straight, but are sometimes helical or curved, whereas S2^1 faults are in general straight. NNW–SSE,

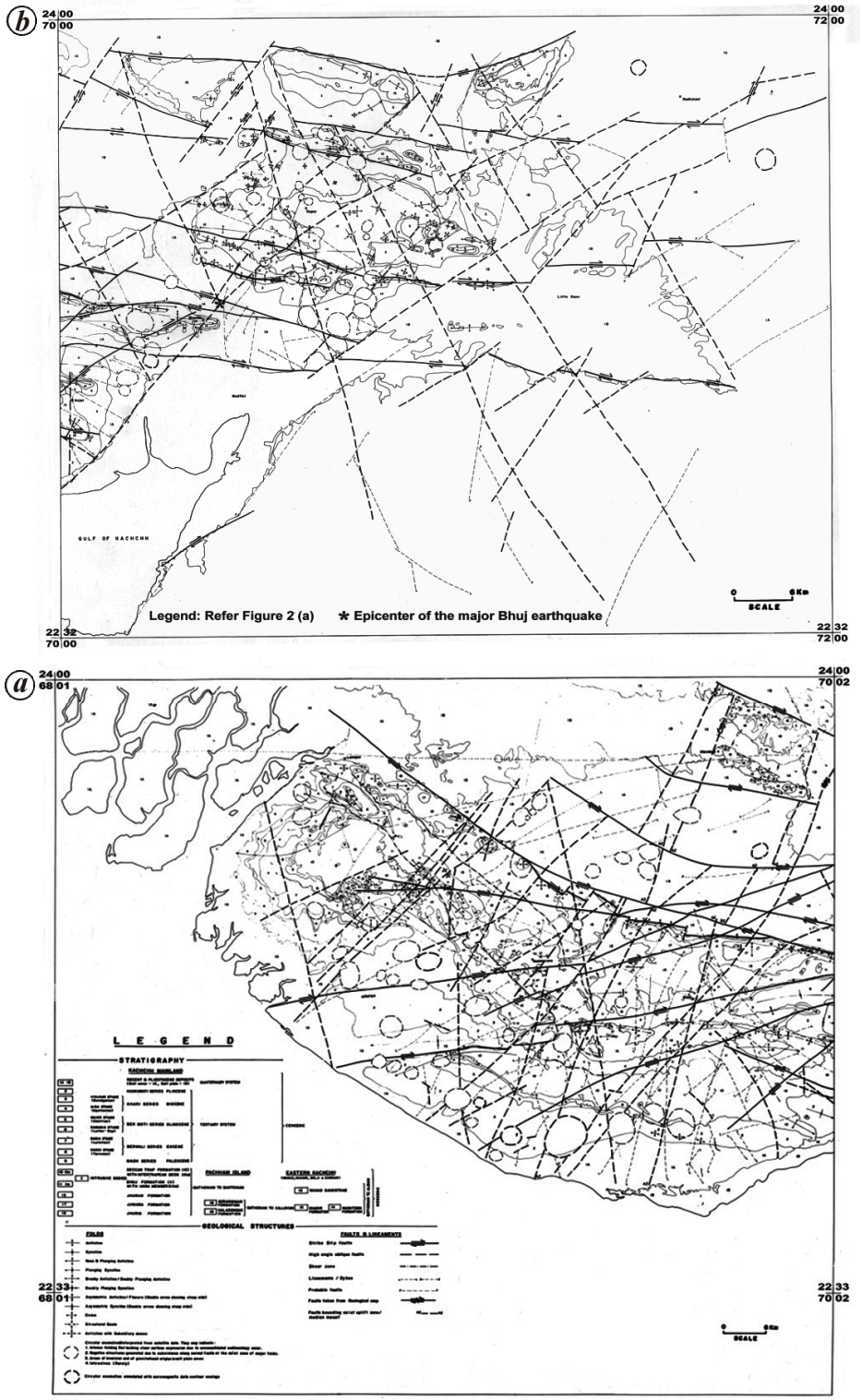

Figure 2. Geological structures and tectonic trends interpreted from IRS-1C (LISS-III) data for (***a***) the western part and (***b***) the eastern part of the study area.

NNE–SSW and N–S trends were also observed in some places. In the Kutch synclinal structure, NNE–SSW trend faults along axial region, displaced at strike–slip boundaries, were mapped representing median massif. Based on the strike–lip faults and their extensions, the Kutch region can be divided into Kutch mainland area, Banni–Lakhadia area, East Banni–Wagad area and Island Belt area, from south to north.

Aeromagnetic data acquisition, processing and interpretation

The regional aeromagnetic data flown at an altitude of 5000 ft amsl along N–S flights with a flight line spacing of 2000 m during 1995, were used in the present study. Cesium vapour magnetometer was employed as the main equipment on-board the aircraft for recording the total intensity of the earth's magnetic field with a sampling rate of 0.25 sec, leading to approximately 25 m ground sampling, with an accuracy of 0.001 nT. The navigation system used was a Trimble TNL-2000A Global Positioning System. TRT radio altimeter was also employed on-board for maintaining the required terrain clearance. Diurnal corrections were applied to the on-board aeromagnetic data by selecting the appropriate reference magnetic level. The differences in the magnetic field values at the points of intersection of each of the tie lines with those of the flight lines were then corrected during tie-line corrections for removing the effects of monthly shift in magnetic levels and the residuals leftover after diurnal corrections. Tie-line corrected data were then corrected for the earth's model field, i.e. International Geomagnetic Reference Field (IGRF), by selecting the appropriate epoch (1995) for enhancing the crustal magnetic anomalies, gridded with a grid cell size of 400 m (1/5th of the flight line spacing) and contoured with a contour interval of 20 nT. As the aeromagnetic data comprise information from subsurface geological strata lying at different depths and are reflected as a cumulative effect, the IGRF corrected data were further subjected to regional–residual separation and computation of second vertical derivatives (SVDs) in order to emphasize the contributions of relatively shallow features and to resolve the overlapping anomalies[12]. SVD maps are presented in Figure 3 *a* and *b* respectively, for the western and eastern portions of the study area.

As the Kutch basin is comprised of non-magnetic Mesozoic and Tertiary sediments, the magnetic response is mainly attributed to the sources in the basement, except where there are extensive Deccan Trap flows either within the sediments or on the surface[21,22]. Therefore, the prime requirement is to compute basement depths for every structure interpreted from aeromagnetic and remote sensing data as well as the same structure at different locations, i.e. to obtain more depths, which are single solutions but not clusters. Though several techniques have been developed during the past few decades for basement depth determination having their own advantages and limitations[23,24], the Peter's half slope method[25–29] is still popular due to its widespread applicability, simplicity and reliability in manual interpretation. It is one of the best methods for aeromagnetic data over sedimentary basins, where depth to the basement is the prime criteria[30,31] and is extensively used in oil exploration work[32]. Hence the basement depths were computed using Peter's method along the flight lines guided by the stacked profiles and then reduced to mean sea level (Figure 4). Out of 169 wells drilled over Peace river, Alberta, Canada the basement depths from flight level computed using this method had an average error of 7.4% with a standard deviation of 6.5% (ref. 27). The basement depths obtained from the above were also validated by the data provided by ONGC and also using the interpretation software over well-defined and un-clustered magnetic anomalies[20,33]. It is to be noted that the basement depth/sediment thickness may vary with the input data used for computations[34]. As the aeromagnetic data were used in this case, it is effectively the 'magnetic basement' and may not necessarily be the geological basement.

Faults were interpreted based on dislocations of the linear anomaly trends or abrupt changes in the anomaly type and pattern, or changes in the background level of the magnetic field. The linear features without clear dislocations, magnetic gradients and alignment of anomalies were interpreted as magnetic trends or lineaments[12,33]. Igneous intrusions usually produce domal structures in the sedimentary strata and all such intrusions were identified. Interpretation of aeromagnetic data has brought out seven distinct magnetic zones, namely A, B, C, D, E, F and G, by outlining the areas of well-defined magnetic anomalies (Table 1 and Figure 5).

Magnetic zone A comprises the westernmost part of the Kutch basin, characterized by short wavelength, weak amplitude and poor anomaly density depicting the typical response of Deccan Trap flows. The pattern of the magnetic anomalies in this zone appears circular in shape.

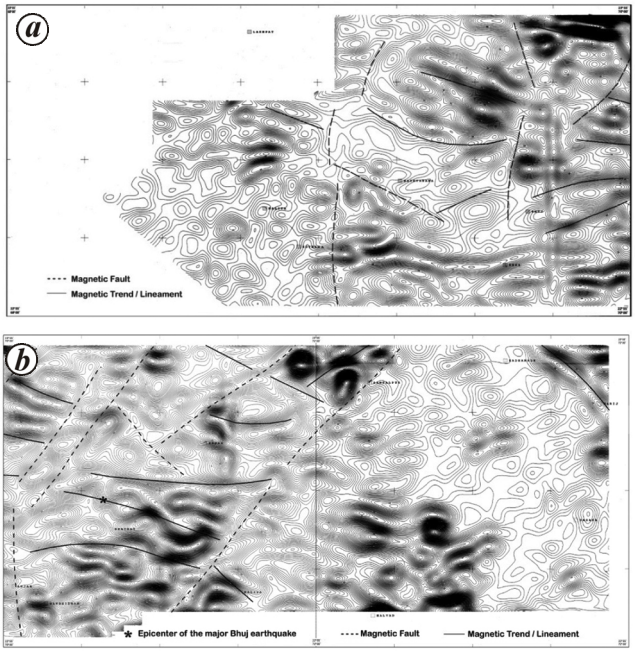

Figure 3. Second vertical derivatives of aeromagnetic data for (***a***) the western part and (***b***) the eastern part of the study area.

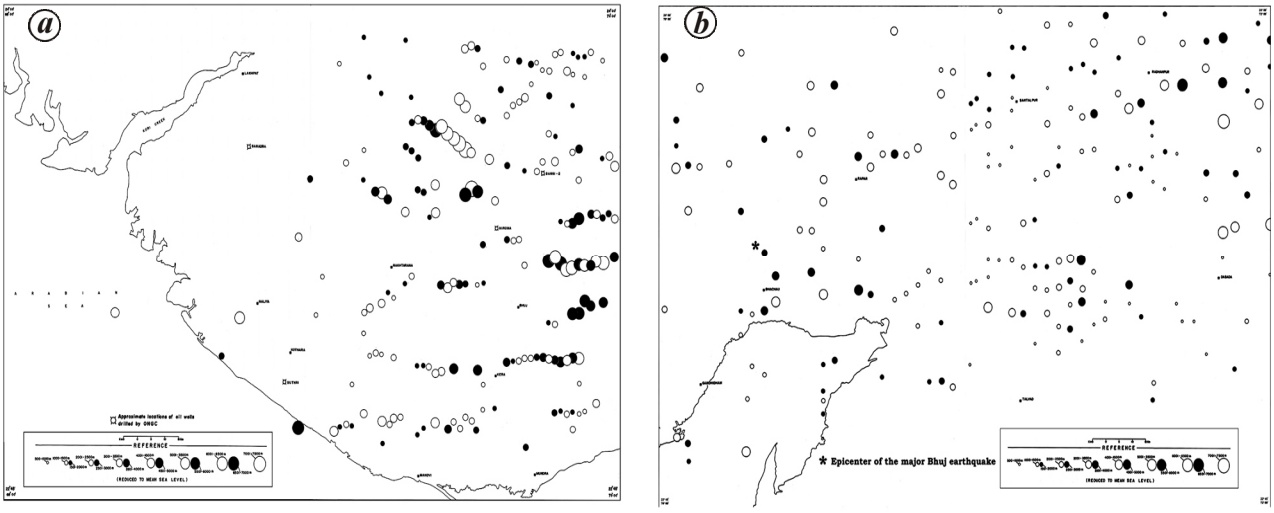

Figure 4. Magnetic basement depth map for (***a***) the western part and (***b***) the eastern part of the study area.

Though the Deccan Traps are exposed only at Sanadra, the magnetic map shows its extension even below Tertiary and Quaternary sediments, by estimating the depths ranging from a few metres to hundreds of metres (Figures 4 *a*, 5 *a* and 6 *a*). The basement depth is more at some places, particularly those parallel to the coastline, i.e. from the southwest of Naliya to the western side of Suthri, the Deccan Traps exist at a depth of about 1500–2000 m. In this zone, extensive flows of Deccan Traps act like a shield for masking the effect of deep basement features. However, the magnetic data helped us estimate the basement depths at two places where the influence of Deccan Traps is perhaps negligible. The first one is at about 8000 m away in the southwestern portion of Naliya in Quaternary sediments towards the coast, where the estimated basement depth is of the order of 5500 m. The second location is in the offshore area situated at about 20,000 m south of Kothara, where the estimated basement depth is of the order of 6500 m. The magnetic lineament trending WNW–ESE at the contact of the Bhuj Formation with the Deccan Traps is nearly parallel to the strike–slip fault interpreted from satellite data. The eastern boundary of this zone is marked by a sharp N–S magnetic break in the magnetic anomaly pattern indicating a N–S magnetic fault, which also appears to continue towards north in the NE direction up to the boundary. The N–S trending fault is segmented into three parts, of which the south and middle parts are in N–S direction and the northern part is in NNE–SSW direction. Among these three segments of this major fault, as evidenced from both magnetic and satellite data, the northern segment is displaced to the east along WNW–ESE trending strike–slip faults, and the central/middle segment of the basin is displaced to the west by ENE–WSW trending strike–slip faults.

Magnetic zone B is characterized by large wavelength and weak amplitude anomalies confined between well-defined zone boundaries (Figures 5 *a* and 6 *a*). The northern boundary of this zone is represented by a strong magnetic gradient trending in the E–W direction, which is close to the major strike–slip fault (north of Nakhtarana) on the northern side of the Kutch mainland, as interpreted from satellite data. The southern and southeastern boundary is well represented by a long magnetic lineament (south of Nakhtarana) trending in the ENE–WSW direction and is parallel to the segment of S2 strike–slip fault, interpreted from remote sensing data. The ENE–WSW direction strike–slip fault shows a break and shift at 69°20′E long. There exist a number of fault segments aligning along this long magnetic lineament. Within the central portion of this zone, the basement high strikes E–W around Nakhtarana and changes its strike to the NW–SE direction in the western part, and is in-line with Lakhpat. This zone is named after the local villages as ‘Nakhtarana–Lakhpat block’ and represents the basement high. The zone ends abruptly at the N–S magnetic break on the eastern side. It is a highland area and occupies only a portion of the western part of the Kutch mainland. Integrated interpretation of aeromagnetic and satellite data suggests a single compound strike–slip fault (above referred two major strike–slip faults) which has been displaced by N–S trending high-angle faults near the margin of this block. The southwestern boundary of this zone is represented by a moderate magnetic gradient extending in the WNW–ESE direction. The inferred fault at the southwestern boundary of this zone falls in the broad shear zone, as interpreted from satellite data. The basement high along with thickness of the sediments ranging from 1500 to 3000 m is supported by the development of a shear zone in the block, as evidenced from both

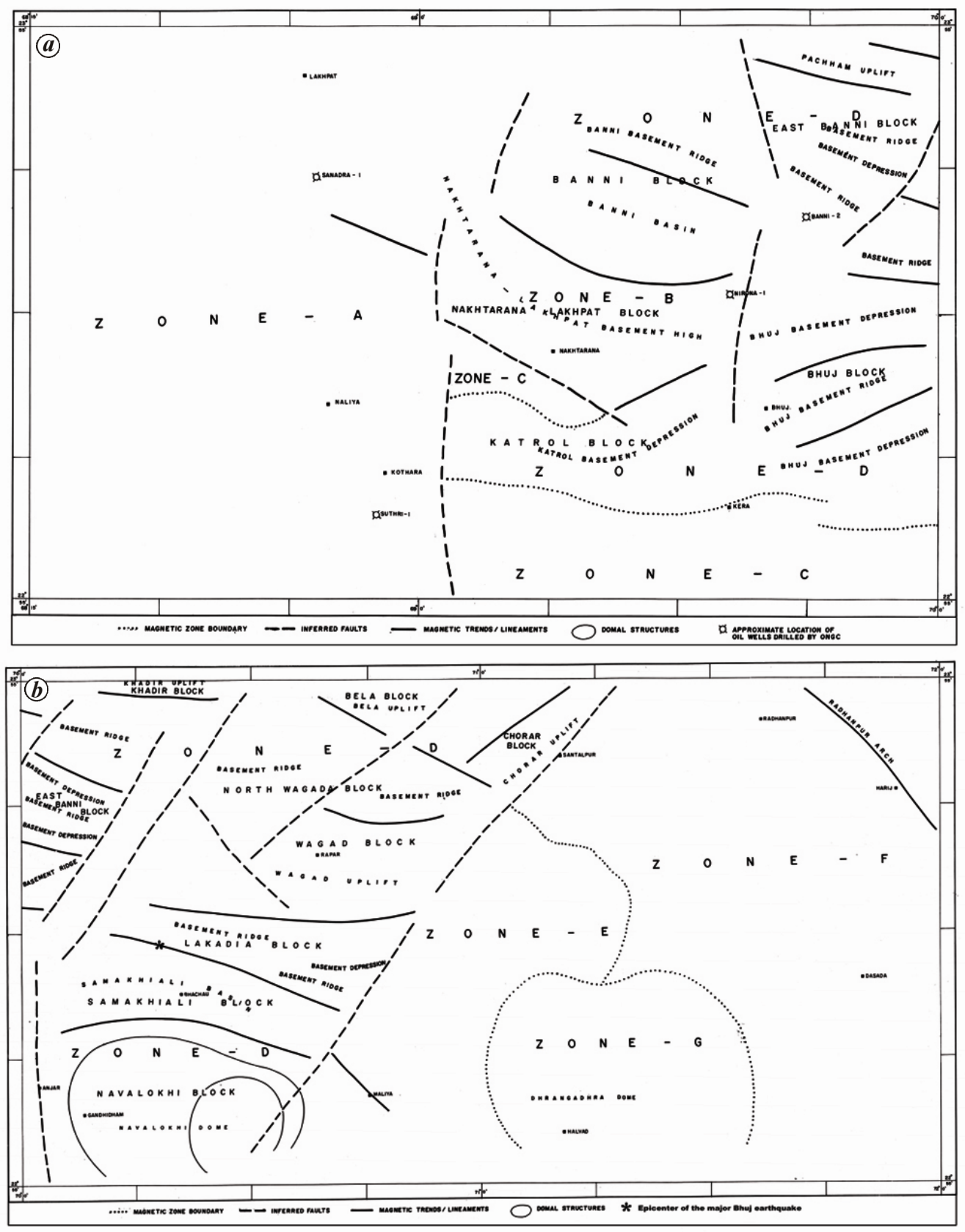

Figure 5. Geological structures and tectonic trends interpreted from aeromagnetic data for (***a***) the western part and (***b***) the eastern part of the study area.

Table 1. Interpretation of different magnetic zones using aeromagnetic data

Magnetic zone	Wavelength	Amplitude	Trend/pattern	Characteristics	Interpretation
A	Short	Weak	Circular	Poor anomaly density	Deccan Trap flows
B	Large	Weak	Well-defined zone boundary	Ends abruptly at magnetic break	Highland
C	Short	Weak	Elongated elliptical anomalies	Interference of magnetic response	Contact of Deccan Traps (Mesozoic) and Tertiary sediments
D	Varying from small to moderate to large	Varying from small to moderate to large	Sharp change in the anomaly pattern	Magnetic axes of the anomalies are discontinuous	Large-scale basement depressions
E	Heterogeneity	Very weak to moderate	Circular to near-elliptical anomalies	Magnetic axes extend from west to east	Possible extension of magnetic basement structure below the Little Rann of Kutch
F	Large	Weak to moderate to weak	Elongated elliptical anomalies in the east and sparse anomalies in the west	Magnetic axis is in the NW–SE direction	Existence of very shallow basement and intra-magnetic basement structures in the western portion and Radhanpur arch in the east
G	Large and short	Large to moderate	Oval-shaped anomalies	Systematic arrangement of anomalies	Domal structure

aeromagnetic and satellite data, within which the thin Bhuj sediment cover has been eroded exposing the older Jhuran Formation in a window NW of Nakhtarana. The complete sequence of Mesozoic sediments of middle Jurassic to Holocene is exposed in this zone. There is one short wavelength weak magnetic anomaly to the west of Nakhtarana, which might be due to the Deccan Traps within the Mesozoic sediments.

Magnetic zone C covers extensive flows of the Deccan Traps and Tertiary sediments located to the south of the Mesozoic sediments situated between 69°00′E and 70°00′E long. It is characterized by short wavelength and week amplitude anomaly response of the Deccan Traps riding over large wavelength anomalies of the basement features under the Tertiary sedimentary cover (Figures 5 *a* and 6 *a*). The boundary of this zone is distinct and exactly follows the contact of the Deccan Traps and Tertiary sediments which extend from east of Kothara to Anjar through Kera, strongly supported by remote sensing data, where the Deccan Traps could be easily seen and mapped. This sub-block is bounded by a series of ENE–WSW trending strike–slip faults and cut across by numerous N–S to NNE–SSW trending high angle faults, as evidenced from satellite data. The eastern and western margins of this zone are bounded by N–S trending faults, as revealed by aeromagnetic and satellite data (Figures 5 and 6). The eastern boundary magnetic lineament could be matched with the western boundary of the median massif zone. The boundary of this zone coincides with the Deccan Traps and is shown with a break (offset) on the western side of Anjar, which coincides with a lineament trending in the NNE–SSW direction. This sub-block of the Kutch mainland is also expected to be a subsidence block having thick sediments. Another important correlation of aeromagnetic and remote sensing data is also observed along the median massif/axial uplift zone of the Kutch synclinal structure. Between Bhuj block of zone D and Nakhtarana–Lakhpat basement high of zone B, a N–S break in magnetic trends is shown as described above, which is the result of inferred fault and is corroborated with satellite data interpretation. Satellite data show the presence of two major faults extending from south to north up to Pachham Island (with displacements along strike–slip faults) trending in NNE–SSW direction, instead of one single fault/magnetic trend as revealed from aeromagnetic data. Therefore, it is concluded that this median massif zone (faults are represented by AZ in map-Figure 6 *a*) is shown as one single magnetic lineament, whereas the same is represented by two major faults in remote sensing data. The E–W magnetic lineaments on either side of these faults also terminate this N–S magnetic fault. From integration of both the datasets, this zone is interpreted as median massif of uplifted block or original basement.

Magnetic zone D spreads over a large central portion of the Kutch basin confined between two well-defined magnetic faults, one on the west trending in the N–S and the other on the east trending in the NE–SW magnetic zone boundaries, marked by a sharp change in the anomaly pattern. The western zone boundary is located to the east

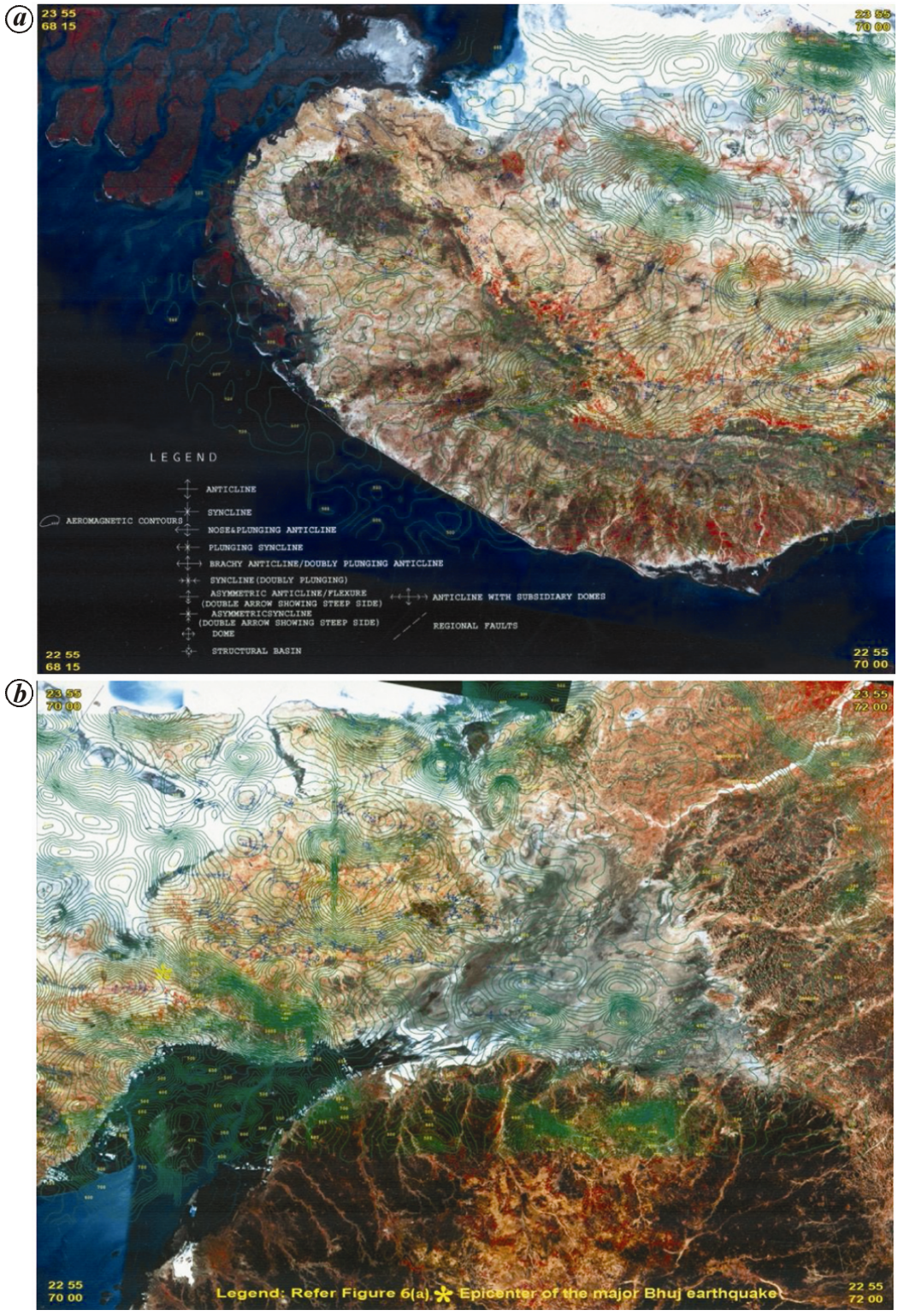

Figure 6. Aeromagnetic (residual) contours and tectonic trends superimposed on IRS-1C (LISS-III) data for (***a***) the western part (***b***) the eastern part of the study area.

of Kothara running across the area from south to north orienting N–S and further swings to NE–SW direction towards north. This fault is described clearly in zone A, as it is segmented into three parts. The eastern side boundary is trending in the NE–SW direction delimiting this zone, and runs across the area from south to north through Santalpur. Within this zone the magnetic axes of the anomalies are discontinuous, orienting in E–W, ESE–

WNW and ENE–WSW directions. This clearly depicts the magnetic basement structural trends under Mesozoic and Quaternary sediments, reflecting a number of magnetic highs and moderate gradients of the magnetic anomalies, which are truncated by N–S and NE–SW faults and were responsible for block faulting of the basement. The basement blocks were uplifted in some cases and down thrown in others, resulting in the formation of a number of basement depressions and ridges. The most striking aeromagnetic anomalies of this zone are located at Banni and Samakhiali blocks respectively, and are characterized by large wavelength and large-scale basement depressions. These depressions (Banni in the north and Samakhiali in the south) are confined between basement faults, as interpreted from aeromagnetic data and strike–slip faults, as interpreted from remote sensing data respectively. Hence, they may be graben-type of structures and are named as Banni and Samakhiali basins respectively. This magnetic zone has undergone severe tectonic activities and is being truncated on the East by a long magnetic lineament orienting in the NE–SW direction, running across the area from south to north through Santalpur. The E–W trend of zone D is also parallel to the known northern Kathiawar fault, which lies outside the study area in the southern portion. The Katrol depression lying west of the median massif is bounded by ENE–WSW strike–slip faults in the north and south, by the N–S fault near Kothara in the west (both from aeromagnetic and satellite data) and median massif fault in the east, and is represented by folded sedimentary sequence. This is also a part of the Kutch mainland depression. Bhuj subsidence block occurs in the east of the median massif and is bounded by E–W trending strike–slip fault in the north, NNE–SSW trending strike–slip fault in the south, median massif fault in the west and N–S trending fault in the east[20,35,36] (also in corroboration with inferred faults from magnetic and satellite data). Within this subsidence block in the central part, a basement ridge bounded by magnetic lineaments trending in the ENE–WSW direction along with depressions on either side is interpreted from magnetic data. This Bhuj basement ridge is the uplifted block along with folded sedimentaries along ENE–WSW strike–slip faults (S2) followed by subsidence on either side. The East Banni basin and Lakhadia block (basement ridge) are bounded by nearly E–W trending magnetic lineaments in the north and south, and inferred faults along NE–SW in the east to N–S faults in the west. All these inferred faults and magnetic lineaments are in corroboration with segments of high-angle faults in the NE–SW to N–S direction and strike–slip faults trending in the E–W direction, as interpreted from satellite data. The basement ridges are the uplifted blocks along with folded sedimentaries. The East Banni block falls in East Banni–Wagad area bounded by strike–slip faults in the north and south, as interpreted from remote sensing data. The western part of the East Banni block is falls in the median massif zone. Hence, this part of the basin is expected to have shallow basement. These magnetic lineaments and inferred faults coincide with trends of segments of strike–slip faults and high-angle oblique faults, as deduced from remote sensing data. This block is covered by salt plains (Figures 5 *b* and 6 *b*). This subsidence block along with folded sediments must have been uplifted, resulting in the formation of ridge and depression based on aeromagnetic data interpretation. The Wagad and North Wagad blocks are also bounded by E–W trending magnetic lineaments and NE–SW trending inferred faults. The magnetic lineaments and inferred faults bounding Pachham, Khadir, Bela and Chorar islands (Island Belt) are in alignment with the fault segments inferred from satellite data, with a southward shift in their location. Another important observation is the presence of Khadir uplift as interpreted from magnetic data, trending in the E–W direction at the northern boundary and WNW–ESE direction at the southern margin, also supported by satellite data.

Magnetic zone E is characterized by very weak to moderate magnetic anomalies with a heterogeneity of magnetic anomalies, which might be due to the possible extension of the magnetic basement structure below the Little Rann of Kutch from zone D. There is a possibility of thin Mesozoic strata in the residual depression of the Little Rann of Kutch. This zone covers part of the Wagad block and Little Rann. Though a NE–SW trending major fault is interpreted on the western margin of zone E adjoining the Wagad block, from both magnetic and satellite data, the lithological and structural continuity of Wagad block into zone E has also been observed (Figure 5 *b*). From aeromagnetic data, the basement is interpreted to continue still further east beyond Wagad into Little Rann. From remote sensing data, it is inferred that the central NE–SW trending regional high-angle fault passes through the middle of zone E, dividing this zone into two parts – eastern and western. The western part, which is in continuity with the Wagad block, is the uplifted block with folded sedimentaries whereas the eastern part is covered by salt plains with sporadic folded Mesozoic exposures.

Magnetic zone F shows weak and sparse magnetic anomalies indicating the existence of basement at a comparatively shallow depth of about 200–1000 m. In this zone, there are a few isolated large wavelength and large moderate to weak amplitude anomalies representing large to moderate-scale intra-magnetic basement structures. The most striking magnetic linear feature in this zone is located to the east of Radhanpur, showing a distinct NW–SE magnetic trend of large magnetic amplitude, and matches well with the known Radhanpur–Barmer arch covered with Quaternary sediments. The depth to this structure was computed as 5000–6000 m. There are two moderate-scale magnetic basement structures located south of Radhanpur in this zone, one each in the north and south of Dasada respectively.

Magnetic zone G exactly matches with the known 'Dhrangadhra dome/Dhrangadhra block', and is characterized by a typical magnetic response of both large wavelength with large amplitude and short wavelength of moderate amplitude, representing moderate magnetic features. The arrangement of magnetic anomalies appears to be nearly oval in shape. The systematic arrangement of magnetic anomalies clearly indicates a domal structure covered with Mesozoic sediments. Within this structure, the magnetic axes are trending in perfect E–W direction. The average depth to these magnetic structures was estimated at 2500–3500 m.

Results and discussion

The quality of interpretation is usually controlled by the degree to which each individual anomaly is free from interference of its neighbours. For realistic interpretation, the best support comes from independent sources. For example, when a fault is interpreted to be nearly outcropping from a magnetic survey, a coincident ill-defined lineament on a satellite image gains new significance. The interpretation of aeromagnetic and satellite data was therefore integrated and the following results were drawn:

(i) The central portion of the Kutch basin had undergone intense tectonic activity and was followed up by intensive magmatism.

(ii) A number of discontinuous large-scale basement structures such as basement highs, ridges, depressions and basins were delineated[37,38].

(iii) The whole Kutch region showed pericontinental rift structures, and had experienced both horizontal and vertical tectonics[39].

(iv) Formation of conjugate set of faults, i.e. strike–slip faults in the E–W direction and high-angle oblique faults in the NE–SW direction took place due to horizontal tectonics. These faults divided the whole region into rhombic-shaped or parallelogram-faced blocks exhibiting block faulting.

(v) Another set of conjugate faults in the ENE–WSW direction and high-angle oblique faults in the NW–SE direction was also observed.

(vi) A long, narrow, conspicuous anomalous zone trending in the NE–SW direction separated the East Banni and North Wagad blocks, and was supported by the abrupt truncation of magnetic lineaments against this zone on either side.

(vii) Major fold trends associated with strike–slip faults were arranged in enechlon pattern and were parallel or little oblique to the direction of the strike–slip faults in a relatively narrow zone surrounding the above faults.

(viii) Though the Navalokhi structure is located at a shallow depth of about 1500 m, it may also hold tectonic significance.

(ix) Wide zones of contemporaneous faulting and enechlon folding development produced by convergent strike–slip faults are important for petroleum exploration, as they form potential traps for hydrocarbon deposits.

(x) The computed basement depths were in good agreement with the results of the wells drilled by ONGC at Nirona-1 and Banni-2 (https://www.google.co.in/?gfe_rd=cr&ei=TDJ5VcuuCerI8AeLrLmoCg&gws_rd=ssl#q=Kutch++geological+maps).

(xi) The basement depth maps could be utilized as a guide to know the approximate thickness of the Tertiary sediments in the basin, useful for estimating the hydrocarbon reserves.

(xii) The basement was at a shallow depth in the eastern portion of the basin.

Based on the above, the following locations are recommended for hydrocarbon exploration:

(i) Banni and Samakhiali basins, based on the thickness of Tertiary sediments of the order of 6000 m and 4000 m respectively.

(ii) The north Bhuj depression may also be considered based on the indicative thickness of Tertiary sediments of approximately 5000 m.

(iii) Circular spectral anomalies interpreted from remote sensing data correlated well with those of the aeromagnetic nosings, which indicates the presence of anomalous deep-rooted subsurface features, especially those observed in Tertiaries adjacent to the strike–slip fault on the western side of Nakhtarana at a distance of 30 km.

(iv) Fold patten in Mesozoic sediments, which are aligned parallel to the northern boundary strike–slip fault of the Kutch mainland on north of Nakhtarana at a distance of approximately 25 km.

(v) Fold pattern in Mesozoic and Tertiary sediments in the southern portion of Rapar from a distance of 15 km onwards.

(vi) Numerous folds developed parallel to strike–slip faults in Mesozoic sedimentaries of the northwestern portion of Anjar at a distance of 15 km to the west of Bhachau.

It was observed that the epicentre of the major earthquake of Bhuj (2001) was located on the ENE–WSW master fault interpreted from magnetic data, corroborated by the strike–slip fault interpreted from satellite data in the same direction, running across the Kutch basin at a shallow depth of approximately 25 km. However, this fault was shifted up and down by transverse tear faults running in the N–S to NE–SW directions. As this strike–slip fault run close to Bhuj and Bhachau, these areas were damaged severely. Three of the aftershocks were located close to the faulted junctions, due to which the areas around Anjar and Rapar were also damaged. It was also observed that all the epicentres of the aftershocks fell in the central portion of the Kutch mainland, which had earlier undergone intense tectonic activity. The stress that could have

caused this major earthquake may be due to the Indian plate pushing northward into the Eurasian plate, resulting into re-activation of this portion of Kutch once again and subsequent re-adjustment of the basement blocks[39]. The interpretation based on the analysis of seismic data reveals that the NW–SE and NE–SW-oriented faults were the causative faults for triggering the above earthquake as severe and prolonged seismic activity was noticed all along the above trends, coinciding with Anjar–Rapar and Bhachao lineaments respectively, in addition to a minor N–S lineament near Anjar[1]. However, in the present study, we observed that the reactivation of E–W and ENE–WSW strike–slip faults and their intersection with the above-mentioned high-angle oblique faults oriented in the NW–SE and NE–SW directions could have triggered the above earthquake. This discrepancy may be attributed to the poor seismic response from the sub-Trap sections while exploring the Mesozoic rocks below the hard Deccan Traps cover[39].

Conclusion

The rift basin of Kutch is undergoing tectonic inversion from Late Cretaceous till the present, causing neo-tectonic uplifts, complicated folding, thrusting and earthquakes[40]. The Bhuj earthquake is significant from the point of view of earthquake disaster mitigation in India[37]. It is evident from this study that the central portion of Kutch mainland has once again undergone intense tectonic activity resulting in a number of complex geological structures. Therefore, the possibility of earthquake occurrence in future also cannot be ruled out. Hence, ground geophysical surveys such as magnetic, micro-seismic and micro-gravity, besides interferometric studies and GPS observations, need to be carried out all along the above-mentioned master faults in order to assess the accumulation of stress from time to time. It can be concluded that the sedimentary basin of Kutch is comprised of a number of sub-basins, ridges and master faults, and that the basins are important for hydrocarbon prospects whereas the master faults are significant with regard to earthquake vulnerability.

1. Gaonkar, S. G., Study of the epicentral trends and depth sections for aftershocks of the 26 January 2001, Bhuj earthquake in western India. *Proc. Indian Acad. Sci.* (*Earth Planet. Sci.*), 2003, **112**, 401–412.
2. Rajendran, K. *et al.*, The 2001 Kutch (Bhuj) earthquake: coseismic surface features and their significance. *Curr. Sci.*, 2001, **80**, 1397–1405.
3. Misra, K. S., Bhutani, R. and Sonp, R., Aftershocks of 26 January 2001 Bhuj earthquake and seismotectonics of the Kutch region. *Proc. Indian Acad. Sci.* (*Earth Planet Sci.*), 2003, **112**, 385–390.
4. Biswas, S. K., The Miliolite rocks of Kutch and Kathiawar (Western India). *Sediment. Geol.*, 1971, **5**, 147–164.
5. Biswas, S. K., Landscape of Kutch – A morphotectonic analysis. *Indian J. Earth Sci.*, 1974, **1**, 177–198.
6. Biswas, S. K., Regional tectonic framework, structure and evolution of the western marginal basins of India. *Tectonophysics*, 1987, **135**, 307–327.
7. Biswas, S. K. and Deshpande, S. V., Basement of the Mesozoic sediments of Kutch, Western India. *Bull. Geol., Min. Metall. Soc. Ind*., 1968, **40**, 1–7.
8. Biswas, S. K. and Deshpande, S. V., Geological and tectonic maps of Kutch. *Bull. ONGC*, 1970, **7**, 115–116.
9. Biswas, S. K. and Deshpande, S. V., A note on mode of eruption of Deccan Trap lavas with special reference to Kutch. *J. Geol. Soc. India*, 1973, **14**, 134–141.
10. Deshpande, S. V., Precambrian basement configuration of Saurashtra Peninsula, W. India. In Proceedings of Symposium on Indian Lithosphere, Centre for Mathematical Modeling and Computer Simulation, Bangalore, 1982, p. 49.
11. Merh, S. S., *Geology of Gujarat*, Geol. Soc. Ind., 1995, p. 222.
12. Rama Rao, B. S. and Murthy, I. V. R., *Gravity and Magnetic Methods of Prospecting*, Arnold – Heinemann Publications, 1978, pp. 285–353.
13. Reeves, C. V., Towards a magnetic anomaly map of reconstructed gondwana. In Ninth International Gondwana Symposium, Hyderabad, 1994, vol. 2, pp. 963–969.
14. Reeves, C. V., Aeromagnetic surveys: principles, practice and interpretation. Course Unit i.50, Postgraduate Diploma and Master of Science programmes in Exploration Geophysics, ITC, The Netherlands, 1996, vol. 1, p. 94.
15. Chandrasekhar, P. and Seshadri, K., Analysis of remote sensing and aeromagnetic data for identification of the causative factors for the recent micro-seismicity observed in Vanasthalipuram area of Ranga Reddy district, Andhra Pradesh, India. *Curr. Sci*., 2013, **104**, 502–508.
16. Rao, D. P. *et al.*, Oil field detection through remote sensing. NRSA Technical Report submitted to Chairman, ISRO, Hyderabad, 1992, p. 11.
17. Chandrasekhar, P. *et al.*, Regional geological studies over parts of Deccan Syneclise using remote sensing and geophysical data for understanding hydrocarbon prospects. *Curr. Sci.*, 2011, **100**, 95–99.
18. Ground water prospects mapping for Rajiv Gandhi National Drinking Water Mission, Project Manual; NRSA Technical Report No. NRSA/RS&GIS-AA/ERG/HGD/TECHMAN/JAN08, 2008, p. 256.
19. Remote sensing applications, Training Lecture Notes, NRSC, Hyderabad, 2009, 203–215.
20. Aeromagnetic survey – interpretation with IRS data in structural mapping for hydrocarbon exploration over Kutch Basin, Gujarat. NRSA Technical Report No. NRSA.AD.44.TR-1/1998, 1998, p. 112.
21. Exploration of sub-trappean Mesozoic basins in the western part of Narmada–Tapti region of Deccan Syneclise, sponsored by Oil Industry Development Board, Ministry of Petroleum & Natural Gas, Govt. of India. NGRI Technical Report No. NGRI-2003-Exp-404, NGRI, 2003, p. 318.
22. Structural and geomorphological mapping in relation to hydrocarbon prospects in parts of Narmada – Tapti lineaments, Maharashtra. NRSA Technical Report, NRSA, 2004, p. 13.
23. Salem, A. and Ravat, D., A combined analytic signal and Euler method (AN-EUL) for automatic interpretation of magnetic data. *Geophysics*, 2003, **68**(6), 1952–1961.
24. Stavrev, P. and Reid, A., Degrees of homogeneity of potential fields and structural indices of Euler deconvolution. *Geophysics*, 2007, **72**(1), L1–L12.
25. Peters, L. J., The direct approach to magnetic interpretation and its practical application. *Geophysics*, 1949, **14**, 290–320.
26. Rao, D. A. and Babu, H. V. R., On the half-slope and straight-slope methods of basement depths determination. *Geophysics*, 1984, **49**, 1365–1368.

27. Nettleton, L. L., *Elementary Gravity and Magnetics for Geologists and Seismologists*, SEG Monograph Series, 1971, vol. 1, pp. 83–87.
28. Telford, W. M., Geldart, L. P. and Sheriff, R. E., *Applied Geophysics*, Cambridge University Press, 1998, 2nd edn, p. 770.
29. Adegoke, J. A. and Layade, G. O., Variation of structural index of Peter's half slope in determining magnetic source-depth. *Arch. Phys. Res.*, 2014, **5**(2), 23–31.
30. Ojo, A. O. *et al*., Determination of location and depth of mineral rocks at Olode village in Ibadan, Oyo State, Nigeria using geophysical methods. *Int. J. Geophys*., 2014, Article ID 306862, pp. 1–13.
31. Anudu1, G. K. *et al*., Analysis of aeromagnetic data over Wamba and its adjoining areas in north-central Nigeria. *Earth Sci. Res.*, 2012, **16**, 25–33.
32. Nettleton, L. L., *Gravity and Magnetics in Oil Prospecting*, McGraw-Hill, 1976, p. 464.
33. Radhakrishna Murthy, I. V., Magnetic interpretation in space domain. In Second SERC School on Geomagnetism and Earth's Interior – Geopotentials-1, Sponsored by the Department of Science and Technology, Government of India, Lecture Notes, 1992, pp. 33–62.
34. Chopra, S. *et al.*, Estimation of sedimentary thickness in Kachchh basin, Gujarat using sp converted phase. *Pure Appl. Geophys.*, 2010, **167**(10), 1247–1257.
35. Chandrasekhar, D. V. *et al.*, Analysis of gravity and magnetic anomalies of Kachchh rift basin, India and its comparison with the New Madrid seismic zone, USA. *Curr. Sci.*, 2005, **88**, 1601–1608.
36. Mishra, D. C., Chandrasekhar, D. V. and Singh, B., Tectonics and crustal structures related to Bhuj earthquake of 26 January 2001: based on gravity and magnetic surveys constrained from seismic and seismological studies. *Tectonophysics*, 2005, **396**, 195–207.
37. Ravi Shanker, Seismotectonics of Kutch rift basin and its bearing on the Himalayan seismicity. *ISET J. Earthq. Technol.*, 2001, **38**, 59–65.
38. Biswas, S. K., Western rift basin of India and hydrocarbon prospects. *J. ONGC*, 1982, 223–232.
39. Biswas, S. K., A review of structure and tectonics of Kutch basin, western India, with special reference to earthquakes. *Curr. Sci*., 2005, **88**, 1592–1600.
40. Biswas, S. K., Status of petrolem exploration in India. *Proc. Indian Natl. Sci. Acad*., 2012, **78**, 475–494.

ACKNOWLEDGEMENTS. We thank D.G.H., New Delhi for funding the aeromagnetic project. P.C. and K.C.M. thank Dr A. Bhattacharya, Mr. M. Suryanarayana, Mr. M. V. V. Kamaraju and officials of DA (A) and IA & I groups of NRSC, Hyderabad for help. P.C. also thanks Prof. I. V. Radhakrishna Murthy (Andhra University); Dr. Y. V. N. Krishna Murthy (Director-NRSC); Mr V. Raghu Venkataraman and Mr D. Vijayan of NRSC for support.

Received 4 February 2016; revised accepted 10 June 2017

doi: 10.18520/cs/v114/i01/74-185